Hindawi Publishing Corporation
International Journal of Polymer Science
Volume 2015, Article ID 871345, 8 pages
http://dx.doi.org/10.1155/2015/871345

Research Article

Optimized Monitoring of Production of Cellulose Nanowhiskers from *Opuntia ficus-indica* (Nopal Cactus)

Horacio Vieyra,[1] Ulises Figueroa-López,[1] Andrea Guevara-Morales,[1] Berenice Vergara-Porras,[1] Eduardo San Martín-Martínez,[2] and Miguel Ángel Aguilar-Mendez[2]

[1]*Instituto Tecnológico y de Estudios Superiores de Monterrey, Carretera Lago de Guadalupe, Km. 3.5, Colonia Margarita Maza de Juárez, 52926 Atizapán de Zaragoza, Mexico*
[2]*Centro de Investigación en Ciencia Aplicada y Tecnología Avanzada, Instituto Politécnico Nacional, Legaria 694, Colonia Irrigación, 11500 Ciudad de México, Mexico*

Correspondence should be addressed to Horacio Vieyra; h.vieyra@itesm.mx

Received 5 September 2015; Accepted 8 November 2015

Academic Editor: Arthur J. Ragauskas

Preparation of cellulose nanowhiskers (CNWs) has grown significantly because they are useful for a wide range of applications. Additional advantage in their design requires that they meet the following characteristics: nontoxicity, abundance, sustainability, renewability, and low cost. To address these requirements, nanowhiskers were prepared from *Opuntia ficus-indica* (nopal) cellulose by acid hydrolysis. Monitoring the process of CNWs preparation is necessary to ensure maximum yield and purity of the end product. In this study, the cellulose preparation was monitored by analyzing microscopic morphology by SEM; the purity degree was determined by fluorescence microscopy as a novel and rapid technique, and FTIR spectroscopy was used for confirmation. The additional parameters that monitored the process were the crystallinity index by X-ray diffraction and the size of the particle by dynamic light scattering (DLS). Nopal cellulose was found to be comparable to commercial microcrystalline cellulose. The use of *Opuntia ficus-indica* is a viable alternative for the production of highly pure CNWs and the strategy to supervise the preparation process was rapid.

1. Introduction

Cellulose, the most abundant biopolymer, is a polysaccharide consisting of a long chain of D-glucose repeat units. Cellulose nanowhiskers (CNWs) are crystalline nanoparticles with a cylindrical shape typically obtained by acid hydrolysis of cellulose fibers whose length is of approximately 100–500 nm with 2–60 nm of diameter [1]. Cellulose nanowhiskers are good candidates for reinforcing other polymers because of their good mechanical properties such as high strength, low thermal expansion coefficient, and the ability to form highly porous meshes [2]. In addition, CNWs offer the advantage of being obtainable from renewable resources. Currently, cellulose nanoparticles can be obtained from plant cell walls by mechanical or chemical treatments, and the preparation of such nanoparticles is becoming an essential topic for researchers working on cellulose.

Several methods have been used to prepare nanowhiskers, such as enzymatic-mediated production [3] and mechanical disintegration of aqueous dispersion of individual cellulose nanofibers [4], but the most common method is the sulfuric acid hydrolysis [5]. During hydrolysis, esterification of cellulose hydroxyl groups to sulfate groups happens and diagonal cleavage of the cellulose happens primarily in the amorphous zone of the fiber releasing needlelike monocrystals referred to as cellulose nanowhiskers. Whisker dimensions and their properties depend on both the origin of the cellulose and reaction conditions employed (i.e., hydrolysis temperature, time, and ultrasonic treatment duration).

Cellulose fibers have been successfully used to reinforce oil-derived polymers [6]. These new formulations of cellulose nanocomposites are suitable for medical purposes because they may mimic the structure of human tissues at the nanoscale due to their rigidity [7, 8].

Reinforcement of synthetic polymers with low cost CNWs may improve the properties of biocompatible polymers to cover a wide range of applications within the biomechanical devices field, to lower production costs and therefore increase accessibility to patients.

Opuntia ficus-indica (nopal) is one of the most widespread and economically important cactus crops. *O. ficus-indica* belongs to the Cactaceae family, *Opuntia* genus, and *Platyopuntia* subgenus. It is a group of arborescent, fleshy-fruited prickly pears from central Mexico [9]. It has elliptic pads (cladodes) that are the source of cellulose and from which CNWs are obtained in this study.

Plant-derived fibers are renewable and abundant and of low cost. Our modern economic system depends on the consumption of natural resources. This is the reason for the shortage of natural resources. Therefore sustainable and reasonable utilization of this kind of resources is a necessity. Moreover, the importance of rationally utilizing nonwood fibers and corn-derived polymers has become increasingly significant due to the highly demanding applications that they already have [10, 11]. Thereby, nopal cellulose meets the criteria: abundance, renewability, and low cost while ensuring the process of purification of crystalline cellulose yielding CNWs suitable for polymer reinforcement.

The aim of this study is the preparation of CNWs using *O. ficus-indica* as the cellulose source and to monitor their production by analyzing the cellulose purity degree by fluorescence microscopy and confirming the size of the particle by dynamic light scattering (DLS) as novel techniques.

2. Materials and Methods

2.1. Preparation of Delignified Nopal Cellulose. Nopal pads (*Opuntia ficus-indica*) were purchased at a marketplace in Mexico City. After the removal of the thorns, the nopal pads were washed with distilled water and disinfected with 1% sodium hypochlorite solution. To remove most noncellulosic constituents, the pads were soaked in a 2% NaOH solution and heated at 70°C for about 20 min. After washing with distilled water, the material was pressed to facilitate the processing of the pulp and fibers. The pressed material was soaked in a 50% v/v solution of H_2O_2 and acetic acid for 4 h for purification and bleaching. Again after washing several times with distilled water, it was oven-dried at 60°C for 24 h. After removing the large fibers, the dried mass (cellulose) was pulverized to obtain a powder or flour (hereafter referred to as raw material) that was sieved through a 150 μm mesh followed by sieving in a 40 μm mesh (CellTrics, Partec, Görlitz, Germany). To remove the remaining lignin, the cellulose powder was dipped into a 2.5 N HCl-5% NH_4OH solution for 60 min at 105°C [12, 13].

2.2. Preparation of Nopal Cellulose Nanowhiskers (NCN) by Acid Hydrolysis. Nopal cellulose nanowhiskers (NCN) were prepared by H_2SO_4-assisted hydrolysis.

Ten grams of nopal cellulose was dispersed in 87.5 mL of an aqueous 64% H_2SO_4 solution after which cellulose hydrolysis was allowed for 4 h at 50°C in a stirring plate. Hydrolysis was interrupted with 400 mL of cold distilled water and the suspension was centrifuged at 3500 rpm and the supernatant was discarded. The sediment was washed three times with cold distilled water until a colloidal suspension was formed, which was sonicated at 60 Hz in a bath sonicator (TI H5, Elma, Rastatt, Germany) [14]. The suspension containing the nanowhiskers was stored at 4°C until it was dried using a freeze dryer (Labconco, Kansas City, MO) at degree of vacuum 0.05 mb and −50°C during 36 h prior analysis and characterization. Commercial microcrystalline cellulose (MCC) 20 μm from Sigma-Aldrich was treated with the same conditions in order to obtain nanowhiskers and compare them with the ones obtained from nopal cellulose.

2.3. Scanning Electron Microscopy. Nopal cellulose particles under 150 μm (raw material) and 40 μm, commercial MCC particles and nanowhiskers from both cellulose types, were analyzed in a scanning electron microscope (JSM-6390LV, JEOL, Japan) with the following settings: 13 kV acceleration voltage, spot size 45, 23 kPa low vacuum, 12 mm of work distance, and magnifications from 27x to 3000x. To improve resolution, some of the samples were sputtered with Au/Pd for 60 s (Desk IV, Denton Vacuum, USA). Samples were observed at high vacuum (HV) at 20 kV, 67 mA, spot size 50, and 11 cm of work distance, at different magnifications.

2.4. Detection of Lignin Content by Fluorescence Microscopy. Epifluorescence microscopy was done using an Axioscope A1 microscope coupled with an HBO100 mercury arc lamp. The sets of filters were blue (excitation: G 365, beam splitter: FT 395, and emission: BP 445/50), green (excitation: BP 470/40, beam splitter: FT 495, and emission: BP 525/50), and red (excitation: BP 587/25, beam splitter: FT 605, and emission: BP 647/70). The image was recorded with an Axiocam MRm monochromatic camera and analyzed with the ZEN Pro software (all from Carl Zeiss, Germany).

2.5. Fourier-Transformed Infrared Spectroscopy. FTIR spectra of nopal cellulose particles under 150 μm, nopal cellulose particles under 40 μm, MCC, untreated dehydrated nopal, and dehydrated nopal films were obtained using an attenuated total reflectance FTIR spectrophotometer (Cary 630 FTIR Spectrometer, Agilent Technologies, Santa Clara, USA). The sample collection was obtained using 32 scans, in the range of 4000 to 500 cm^{-1}, at a resolution of 4 cm^{-1}. Samples were pressed against the objective lens and analyzed directly.

2.6. X-Ray Diffraction. The X-ray diffraction measurements were performed using a Siemens D5000 system (Aubrey, TX) with theta-theta drive goniometer. The diffraction patterns were recorded using a copper K-alpha X-ray source at a voltage of 30 kV and a 20 mA power (=1.5418 Å). The XRD data was collected at 0.05-degree resolution, at 15 seconds of counting time per step, from 10 to 60 degrees (2θ scale).

2.7. Size Measurement by Dynamic Light Scattering. The size of nopal CNWs was determined using Zetasizer Nano ZS

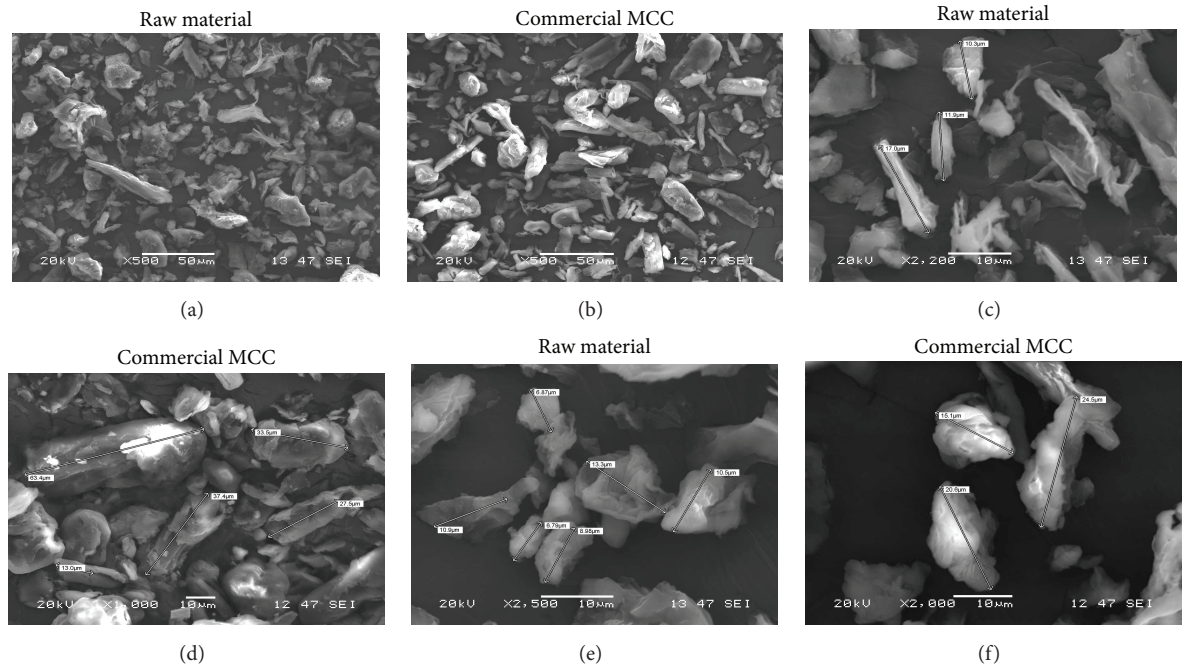

Figure 1: SEM morphological analysis of nopal cellulose microparticles (a, c, e) and commercial microcrystalline cellulose (b, d, f).

ZEN3600 equipment (Malvern Instruments, UK) by measuring the hydrodynamic diameter and polydispersity index by dynamic light scattering (DLS). Size measurements were performed in triplicate, with each measurement conducted using 3 mL of suspension at room temperature (25°C). Mean particle size (z-average) ± standard deviation and an estimate of the width of the distribution (polydispersity index, PdI) were performed by means of analysis of cumulants.

3. Results and Discussion

3.1. Morphological Analysis of Nopal Cellulose Microparticles. Morphology and size distribution of the nopal and the commercial cellulose were similar (Figures 1(a) and 1(b)). Generally, the particle size ranged from 5 μm to 50 μm. Aggregates, round shape, and elongated particles constituted the sheer bulk in both materials as previously described [15], although larger agglomerations were observed in MCC (Figure 1(b)) at 500x. At larger magnifications (Figures 1(d) and 1(f)) the morphology of the commercial cellulose microcrystals was better-defined showing crystals averaging 20 μm. This morphology seems identical to the nopal cellulose microparticles. Although SEM imaging is not conclusive, micrographs indicated that the process of obtaining nopal cellulose could be effective.

3.2. Photophysical Properties of Nopal Cellulose. Nopal cellulose can exhibit photophysical properties depending on the degree of lignin content. Lignin autofluorescence can be detected in the blue range of the fluorescence spectrum under 365 nm excitation (emission between 400 and 450 nm) and the fluorescence extends to the green range beyond 490 nm [16–18]. To evaluate the delignification process, we observed the nopal cellulose with an epifluorescence microscope using blue, green, and red fluorescence detectors as described in Materials and Methods (Figure 2). Before processing, the raw material exhibited autofluorescence in the three fluorescence detectors that were evaluated (left panel); the merge of the three fluorescence images appears at the bottom of each column. After a delignification treatment the autofluorescence of the material disappeared and the delignified nopal cellulose (middle panel) was comparable to the commercial cellulose (right panel). Commercial microcrystalline cellulose was used as control and images were acquired with the same instrument settings.

Lignin fluorescence may be the consequence of charge-transfer mechanisms, distinct molecular species within the lignin polymer (i.e., phenylcoumarone and stilbene structures), and other lignin chromophores that emit fluorescence in both blue and green part of the spectrum [19]. Red fluorescence in the raw was also observed. This may be associated with lignin breakdown products as lignin is made from about 20 multifunctional phenylpropanoid components that absorb different wavelengths producing a complex lignin spectrum. Consequently, the loss of the fluorescence in the delignified nopal cellulose together with the SEM morphological features of the material indicated an acceptable purity degree of cellulose, which would be used to prepare nanowhiskers.

Using autofluorescence to detect lignin has some advantages, including the fact that very small amounts of material are required and the detection is nondestructive; therefore the material can be recovered from the slides. In addition, the results are obtained immediately upon microscope visualization.

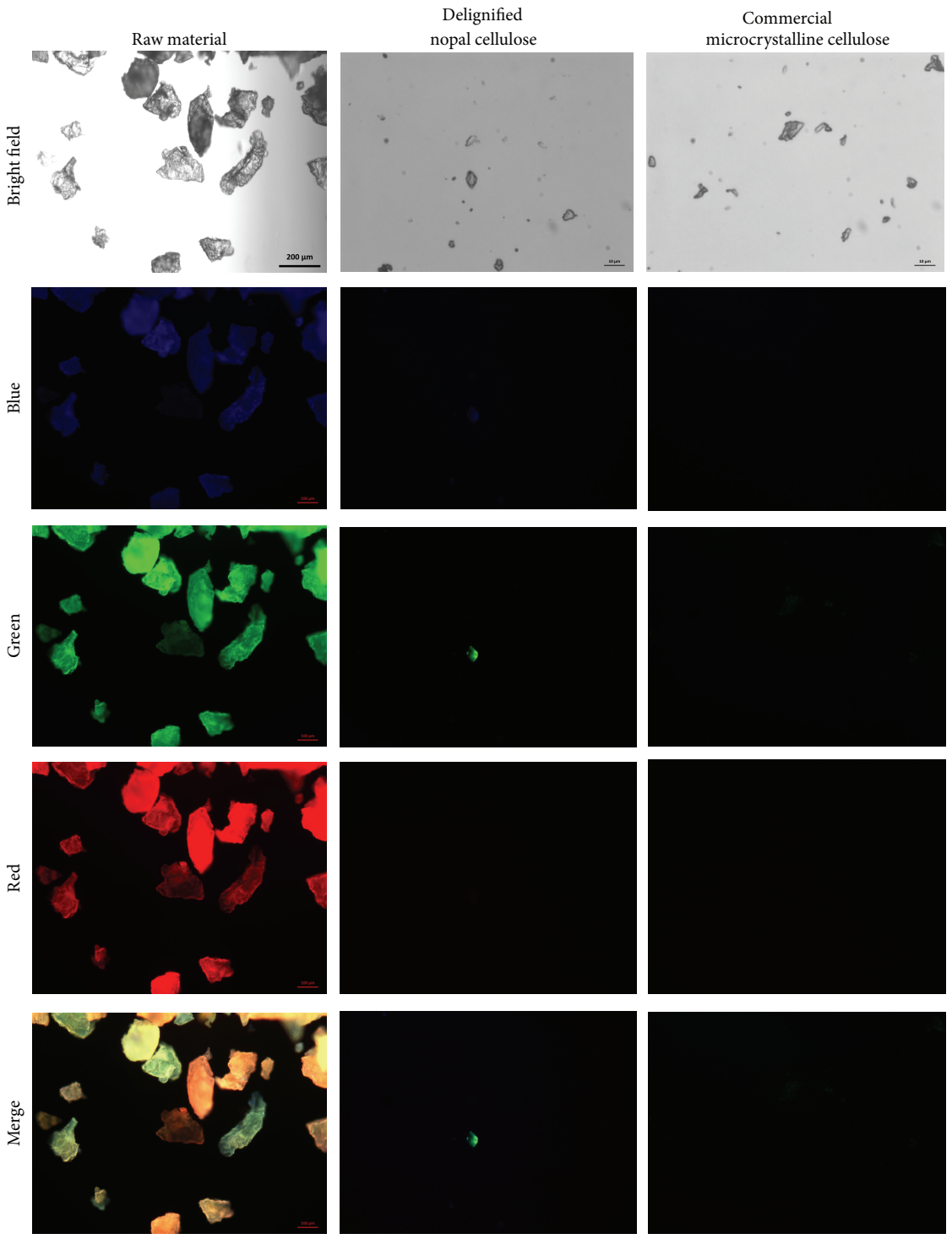

Figure 2: Photophysical properties by epifluorescence microscopy of the nopal raw material, delignified cellulose, and commercial microcrystalline cellulose.

3.3. Fourier-Transformed Infrared Spectroscopy. The morphological and photophysical analysis of the nopal cellulose revealed high similarity between nopal and commercial crystalline cellulose. A FTIR analysis was performed to further confirm the purity of nopal cellulose. Figure 3 showed the comparative spectra. The broad band observed in the three spectra in the range from 3500 cm^{-1} to 3000 cm^{-1} is indicative of O–H stretching vibrations. A slight decreased OH signal intensity at 3300 cm^{-1} was observed in the nopal cellulose likely due to the percentage of cellulose in the sample (in contrast to the pure cellulose of the commercial MCC). The peak at 2868 cm^{-1} is attributed to the aliphatic

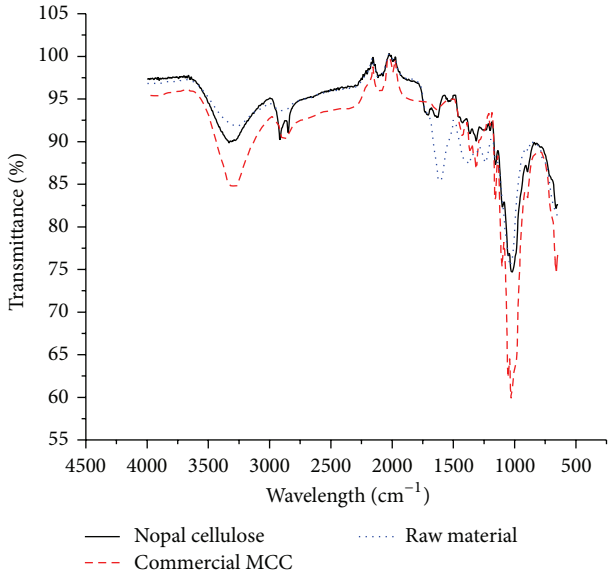

Figure 3: Infrared spectroscopy of raw material, nopal cellulose, and commercial microcrystalline cellulose.

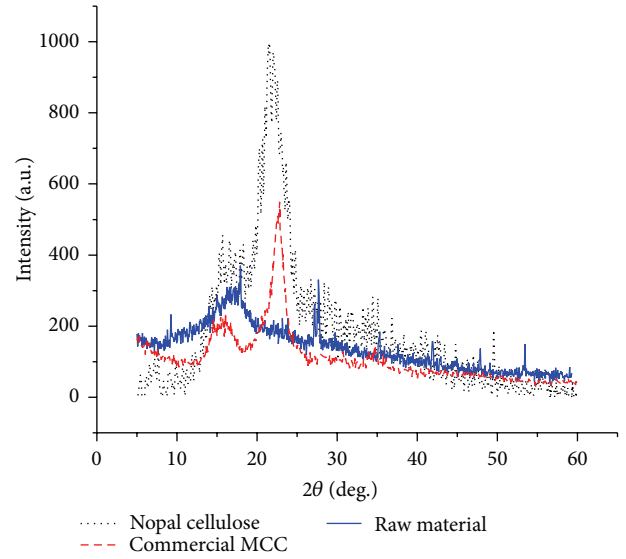

Figure 4: X-ray diffraction patterns of nopal and microcrystalline cellulose.

saturated C–H stretching vibration in cellulose. The native cellulose I_α and cellulose I_β have different O–H stretching and out-of-plane bending bands because of their different hydrogen-bonding strength. The peak of O–H stretching at 3270 cm^{-1} and that of O–H out-of-plane bending at 710 cm^{-1} are simultaneously observed in the spectra of commercial MCC and nopal cellulose, indicating that they both are cellulose type I_β (phase thermodynamically more stable than I_α) [20, 21].

The peak at 1430 cm^{-1} of the commercial MCC assigned to CH_2 bending vibration is also associated with the amount of the crystalline structure of the cellulose [22]. The peaks at the region 1630–1430 cm^{-1} observed in the nopal MCC are indicative of the presence of lignin and attributed to the C–C vibration or to absorbed water (present in the case of bleached and acid treated fibers) [23]. The peak at 1731 cm^{-1} is due to the acetyl and uronic ester groups of residual hemicellulose or to the ester linkage of carboxylic group of the ferulic and p-coumaric acids of lignin [24].

The bands in the region 1250–1400 cm^{-1} comprise the C–O stretching vibrations of aliphatic primary and secondary alcohols in cellulose. The broad peaks at 1050 cm^{-1} are assigned to ether linkage (C–O–C) while the peak at 667 cm^{-1} is due to the out-of-plane bending vibration of intermolecular H-bonded O–H group and out-of-plane O–H bending. Other absorption peaks observed from 1800 cm^{-1} to 600 cm^{-1} are related to the deformation, wagging, and twisting modes of the anhydroglucopyranose unit, which is consistent with previous studies [25, 26].

The main difference among the three FTIR spectra was the band observed at approximately 1600 cm^{-1} in the raw material. This spectrum is similar to the lignin of natural fibers [27]. Thus, the presence of lignin in the raw material, which was chemically untreated, is likely the origin of this band. Cellulose displays characteristic bands at 3496 cm^{-1} (O–H), 1110 cm^{-1} (C–O of secondary alcohol), and 2868 cm^{-1} (C–H from –CH_2) [28]. The bands at 3496 cm^{-1} and 2868 cm^{-1} were conserved in the raw material and nopal cellulose, but the 1110 cm^{-1} peak was decreased in both nopal samples probably because of the difference in purity.

3.4. X-Ray Diffraction. The general cellulose crystallinity is reported between 30 and 80% [29] and indicates the percentage of all the cellulose occupied in the crystalline region. A considerable part of the cellulose structure is less ordered; this part is referred to as amorphous [30]. X-ray diffraction (XRD) provided strong signals from the crystalline fraction of the cellulose. The crystallinity index reported in the literature is highly dependent on the choice of the X-ray instrument, data evaluation procedure applied to the measurement, and the preparation of the sample. The noncrystalline part of the cellulose structure would be represented by broader and less clearly refined features in the diffraction pattern [31].

Diffractograms of the samples are depicted in Figure 4. MCC X-ray diffraction spectrum was the characteristic of powder type I cellulose, whose crystallinity was evident by giving three peaks. The main peak at 2θ 22.5° is indicative of the distance between hydrogen-bonded sheets in cellulose I. There is a broad peak at ~16°, which is known to be a convoluted peak from I_β. The third small peak at 34.5° corresponds to 1/4 of the length of one cellobiose unit and arises from ordering along the fiber direction. The intensity of the peak at 2θ 22.5° in the X-ray diffraction pattern of the nopal microcellulose denoted a higher degree of crystallinity and implied the removal of noncellulosic components.

Cellulose crystallinity is dependent on the data evaluation procedure applied to the measurement and on the experimental mode [32]. In this work, the delignification process eliminated the amorphous components (lignin, hemicellulose) present in the raw material, which lacked crystallinity and appeared to be mainly amorphous. In agreement with the

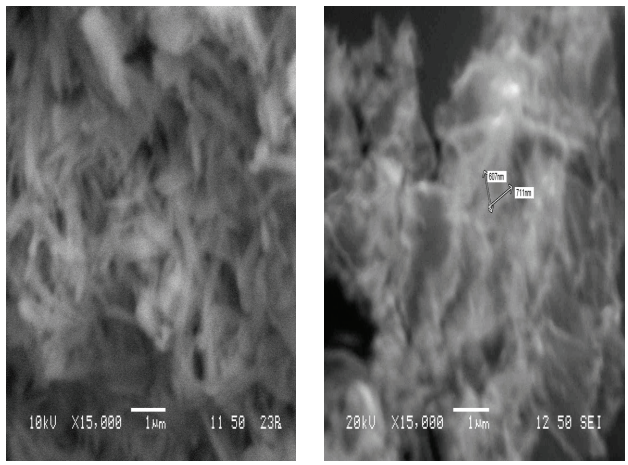

(a) (b)

Figure 5: SEM cellulose nanowhiskers micrographs. (a) Commercial MCC nanowhiskers, (b) nopal CNWs.

loss of autofluorescence and SEM morphological features, the X-ray diffraction analysis indicated the nopal cellulose had a high purity degree.

3.5. Nanowhiskers Obtainment. The principal method for the preparation of nanowhiskers from cellulose fibers is based on acid hydrolysis. Microcrystalline cellulose fibers are comprised of basic fibers with monocrystalline domains linked by amorphous domains. Generally, monocrystalline cellulose has been reported with length ranges from 100 to 500 nm and diameter between 20 and 60 nm [33, 34]. When cellulose fibers are hydrolyzed with 64% (w/v) sulfuric acid, transverse cleavage of the cellulose happens primarily in the amorphous zone of the fiber and releases needlelike monocrystals referred to as cellulose nanowhiskers (CNWs) [35].

The SEM image of CNWs is shown in Figure 5. The length of CNWs prepared from commercial cellulose (Figure 5(a)) ranged from 300 to 800 nm and the diameter from 30 to 80 nm. The whiskers appeared as a homogeneous needlelike material, the material was well dispersed, and no agglomerations were observed. These CNWs were larger than those expected from MCC [5, 36], probably because the length of the nanowhiskers depends on the source of the cellulose as well as on the temperature and overall conditions of the acid hydrolysis [37]. The length of CNWs prepared from nopal cellulose (Figure 5(b)) ranged from 300 to 800 nm and the diameter from 50 to 100 nm. These CNWs had morphological features similar to those prepared from commercial cellulose. Since CNWs appear as needlelike nanoparticles with a relatively high aspect ratio, they are likely to possess a higher reinforcing capability [38, 39] because the roughness and larger exposed surface of the CNWs may improve the mechanical interlacing [40].

3.6. Size Measurement by Dynamic Light Scattering. The z-average is an intensity based calculated value and should never be confused with or directly compared to a mass or number mean value produced by other methods. The

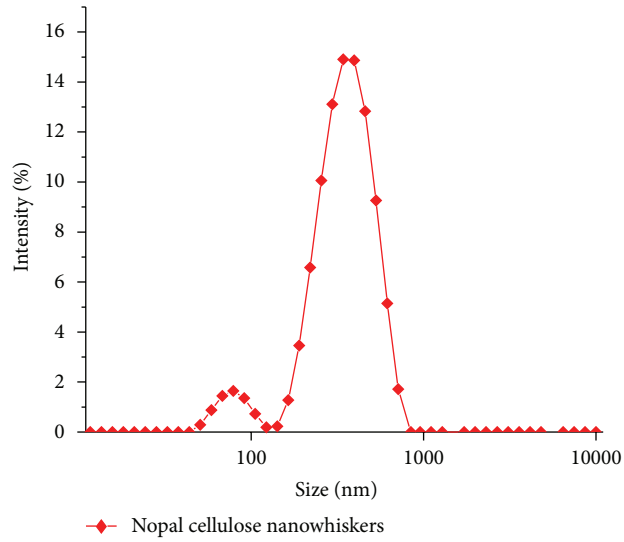

Figure 6: Hydrodynamic size distribution of nopal cellulose nanowhiskers.

polydispersity index is dimensionless and scaled such that values smaller than 0.05 are rarely seen other than with highly monodisperse standards. Values greater than 0.7 indicate that the sample has a very broad size distribution and is probably not suitable for the dynamic light scattering (DLS) technique.

DLS is usually performed in monomodal (i.e., only one peak), spherical, and monodisperse (i.e., no width to the distribution) samples prepared in the correct dispersant. However this technique can be used to measure nonspherical particles [41]. For nonspherical particles, DLS will give the diameter of a sphere that has the same average translational diffusion coefficient as the particle being measured. This size distribution is displayed as a plot of the relative intensity of light scattered by particles (on the y-axis) versus various size classes (on the x-axis) that are logarithmically spaced.

The size distribution plot showed two peaks (Figure 6) and indicated two sizes in the sample: the larger particle

size (z-average, right peak), associated with the length of the nopal CNWs, was 373.7 ± 123 nm and the smaller particle size (z-average of the left peak) was associated with the diameter of the whisker and was 79.7 ± 16.79 nm. The polydispersity index was 0.43 indicating that the size of the material was measurable using this technique and the result met the instrument quality criteria for size measurement [42]. In practice, particles or macromolecules in solution are nonspherical, dynamic (tumbling), and solvated. Because of this, the diameter calculated from the diffusional properties of the particle will be indicative of the apparent size of the dynamic hydrated/solvated particle, hence the terminology, hydrodynamic diameter.

Nopal cellulose nanowhiskers were designed and prepared in this study. The evaluation of the right polymer to be reinforced with this type and size of nanowhiskers depends on the final intended function of the polymer composite. CNWs incompatibility issues and the tendency to form aggregates can be overcome by means of functionalizing the nanowhiskers to improve anchorage of reinforcement to the matrix. Some areas of interest include reinforcement of polymers for biomedical purposes such as PHB (polyhydroxybutyrate), PLA (polylactide), which are biodegradable as cellulose but their mechanical properties are poor [43] compared with the properties of polyethylene, which is not biodegradable. Also, cellulose nanowhiskers with high surface areas would be particularly useful for applications such as green nanocomposites ultrafiltration, biomedicine, and catalyst supports.

4. Conclusions

In this study, nopal CNWs were produced and characterized and microcrystalline cellulose was used as a control. There is a wide range of cellulose sources; the use of *Opuntia ficus-indica* (nopal cactus) is a viable alternative for the production of CNWs. The high purity of the cellulose is necessary for nanowhiskers preparation; here, the fluorescence measurement was presented as a quality control method to assess purity of the raw material. In addition, DLS provided a complementary method for size measurement of nanowhiskers. Due to their morphology, crystallinity, and size, nopal cactus nanowhiskers would have the capability to reinforce biomaterials like PHB polymer for manufacturing purposes.

Conflict of Interests

The authors declare that there is no conflict of interests regarding the publication of this paper.

Acknowledgments

The authors thank Dr. Esmeralda Juárez (INER-Salud Mexico) for her technical assistance and the critical review of the paper. H. Vieyra thanks the National Council of Science and Technology of Mexico (CONACYT) for the fellowship received.

References

[1] R. Dash, M. Foston, and A. J. Ragauskas, "Improving the mechanical and thermal properties of gelatin hydrogels cross-linked by cellulose nanowhiskers," *Carbohydrate Polymers*, vol. 91, no. 2, pp. 638–645, 2013.

[2] S. J. Eichhorn, "Cellulose nanowhiskers: promising materials for advanced applications," *Soft Matter*, vol. 7, no. 2, pp. 303–315, 2011.

[3] P. B. Filson, B. E. Dawson-Andoh, and D. Schwegler-Berry, "Enzymatic-mediated production of cellulose nanocrystals from recycled pulp," *Green Chemistry*, vol. 11, no. 11, pp. 1808–1814, 2009.

[4] X. Cao, B. Ding, J. Yu, and S. S. Al-Deyab, "Cellulose nanowhiskers extracted from TEMPO-oxidized jute fibers," *Carbohydrate Polymers*, vol. 90, no. 2, pp. 1075–1080, 2012.

[5] Y. Li and A. Ragauskas, "Cellulose nano whiskers as a reinforcing filler in polyurethanes," in *Advances in Diverse Industrial Applications of Nanocomposites*, B. Reddy, Ed., pp. 18–36, InTech, Rijeka, Croatia, 2011.

[6] N. Macedo, F. Matuda, L. Macedo, A. Monteiro, M. Valera, and Y. Carvalho, "Evaluation of two membranes in guided bone tissue regeneration: histological study in rabbits," *Brazilian Journal of Oral Sciences*, vol. 3, pp. 395–400, 2004.

[7] M. Koller, A. Salerno, A. Muhr et al., "Synthesis of thermally stable polyesters," in *Polyester*, S. H. El-Din, Ed., pp. 19–60, InTech, 2012.

[8] C. Dahlin, A. Linde, J. Gottlow, and S. Nyman, "Healing of bone defects by guided tissue regeneration," *Plastic and Reconstructive Surgery*, vol. 81, no. 5, pp. 672–676, 1988.

[9] K. El-Mostafa, Y. El Kharrassi, A. Badreddine et al., "Nopal cactus (*Opuntia ficus-indica*) as a source of bioactive compounds for nutrition, health and disease," *Molecules*, vol. 19, no. 9, pp. 14879–14901, 2014.

[10] C. K. Williams and M. A. Hillmyer, "Polymers from renewable resources: a perspective for a special issue of polymer reviews," *Polymer Reviews*, vol. 48, no. 1, pp. 1–10, 2008.

[11] M. S. Sreekala, K. Goda, and P. V. Devi, "Sorption characteristics of water, oil and diesel in cellulose nanofiber reinforced corn starch resin/ramie fabric composites," *Composite Interfaces*, vol. 15, no. 2-3, pp. 281–299, 2008.

[12] M. K. Mohamad Haafiz, S. J. Eichhorn, A. Hassan, and M. Jawaid, "Isolation and characterization of microcrystalline cellulose from oil palm biomass residue," *Carbohydrate Polymers*, vol. 93, no. 2, pp. 628–634, 2013.

[13] L. Aquino, J. Rodriguez, A. M. Mendez, and S. E. Hernandez, "Extraction and characterization of nopal (*Opuntia ficus indica*) fiber," *Naturaleza y Desarrollo*, vol. 10, pp. 46–63, 2012.

[14] M. K. M. Haafiz, A. Hassan, Z. Zakaria, and I. M. Inuwa, "Isolation and characterization of cellulose nanowhiskers from oil palm biomass microcrystalline cellulose," *Carbohydrate Polymers*, vol. 103, no. 1, pp. 119–125, 2014.

[15] V. Jollet, F. Chambon, F. Rataboul et al., "Non-catalyzed and Pt/γ-Al_2O_3-catalyzed hydrothermal cellulose dissolution–conversion: influence of the reaction parameters and analysis of the unreacted cellulose," *Green Chemistry*, vol. 11, no. 12, pp. 2052–2060, 2009.

[16] L. A. Donaldson, R. H. Newman, and A. Vaidya, "Nanoscale interactions of polyethylene glycol with thermo-mechanically pre-treated *Pinus radiata* biofuel substrate," *Biotechnology and Bioengineering*, vol. 111, no. 4, pp. 719–725, 2014.

[17] N. Sathitsuksanoh, B. Xu, B. Zhao, and Y.-H. P. Zhang, "Overcoming biomass recalcitrance by combining genetically modified switchgrass and cellulose solvent-based lignocellulose pretreatment," *PLoS ONE*, vol. 8, no. 9, Article ID e73523, 2013.

[18] K. Radotić, A. Kalauzi, D. Djikanović, M. Jeremić, R. M. Leblanc, and Z. G. Cerović, "Component analysis of the fluorescence spectra of a lignin model compound," *Journal of Photochemistry and Photobiology B: Biology*, vol. 83, no. 1, pp. 1–10, 2006.

[19] B. Albinsson, S. Li, K. Lundquist, and R. Stomberg, "The origin of lignin fluorescence," *Journal of Molecular Structure*, vol. 508, no. 1–3, pp. 19–27, 1999.

[20] M. Wada, T. Kondo, and T. Okano, "Thermally induced crystal transformation from cellulose I_α to I_β," *Polymer Journal*, vol. 35, no. 2, pp. 155–159, 2003.

[21] P. Lu and Y.-L. Hsieh, "Preparation and properties of cellulose nanocrystals: rods, spheres, and network," *Carbohydrate Polymers*, vol. 82, no. 2, pp. 329–336, 2010.

[22] M. Poletto, H. L. Ornaghi, and A. J. Zattera, "Native cellulose: structure, characterization and thermal properties," *Materials*, vol. 7, no. 9, pp. 6105–6119, 2014.

[23] B. M. Cherian, L. A. Pothan, T. Nguyen-Chung, G. Mennig, M. Kottaisamy, and S. Thomas, "A novel method for the synthesis of cellulose nanofibril whiskers from banana fibers and characterization," *Journal of Agricultural and Food Chemistry*, vol. 56, no. 14, pp. 5617–5627, 2008.

[24] X. F. Sun, F. Xu, R. C. Sun, P. Fowler, and M. S. Baird, "Characteristics of degraded cellulose obtained from steam-exploded wheat straw," *Carbohydrate Research*, vol. 340, no. 1, pp. 97–106, 2005.

[25] Y. Li, H. Ren, and A. J. Ragauskas, "Rigid polyurethane foam/cellulose whisker nanocomposites: preparation, characterization, and properties," *Journal of Nanoscience and Nanotechnology*, vol. 11, no. 8, pp. 6904–6911, 2011.

[26] Z. Lu, L. Fan, H. Zheng, Q. Lu, Y. Liao, and B. Huang, "Preparation, characterization and optimization of nanocellulose whiskers by simultaneously ultrasonic wave and microwave assisted," *Bioresource Technology*, vol. 146, pp. 82–88, 2013.

[27] F. Mizi, D. Dasong, and H. Biao, "Fourier transform infrared spectroscopy for natural fibres," in *Fourier Transform: Materials Analysis*, S. Salih, Ed., chapter 3, pp. 45–68, Intechopen, Rijeka, Croatia, 2012.

[28] G. Siqueira, J. Bras, and A. Dufresne, "New process of chemical grafting of cellulose nanoparticles with a long chain isocyanate," *Langmuir*, vol. 26, no. 1, pp. 402–411, 2010.

[29] H. Chen, "Chemical composition and structure of natural lignocellulose," in *Biotechnology of Lignocellulose*, pp. 25–71, Springer, Dordrecht, The Netherlands, 2014.

[30] S. Park, J. O. Baker, M. E. Himmel, P. A. Parilla, and D. K. Johnson, "Cellulose crystallinity index: measurement techniques and their impact on interpreting cellulase performance," *Biotechnology for Biofuels*, vol. 3, article 10, 2010.

[31] N. Terinte, R. Ibbett, and K. C. Schuster, "Overview on native cellulose and microcrystalline cellulose I structure studied by X-ray diffraction (WAXD): comparison between measurement techniques," *Lenzinger Berichte*, vol. 89, pp. 118–131, 2011.

[32] M. Deraman, S. Zakaria, and J. A. Murshidi, "Estimation of crystallinity and crystallite size of cellulose in benzylated fibres of oil palm empty fruit bunches by X-ray diffraction," *Japanese Journal of Applied Physics*, vol. 40, no. 5, pp. 3311–3314, 2001.

[33] S. J. Eichhorn, C. A. Baillie, N. Zafeiropoulos et al., "Current international research into cellulosic fibres and composites," *Journal of Materials Science*, vol. 36, no. 9, pp. 2107–2131, 2001.

[34] W. Helbert, J. Y. Cavaillé, and A. Dufresne, "Thermoplastic nanocomposites filled with wheat straw cellulose whiskers. Part I. Processing and mechanical behavior," *Polymer Composites*, vol. 17, no. 4, pp. 604–611, 1996.

[35] J. R. Araujo, W. R. Waldman, and M. A. De Paoli, "Effect of heat treatment and compatibilizer on properties of polypropylene/sisal fiber composites," *Polymer Degradation and Stability*, vol. 93, no. 10, pp. 1770–1775, 2008.

[36] S. K. Bajpai, V. Pathak, B. Soni, and Y. M. Mohan, "CNWs loaded poly(SA) hydrogels: effect of high concentration of CNWs on water uptake and mechanical properties," *Carbohydrate Polymers*, vol. 106, no. 1, pp. 351–358, 2014.

[37] X. M. Dong, J.-F. Revol, and D. G. Gray, "Effect of microcrystallite preparation conditions on the formation of colloid crystals of cellulose," *Cellulose*, vol. 5, no. 1, pp. 19–32, 1998.

[38] H. Angellier, S. Molina-Boisseau, P. Dole, and A. Dufresne, "Thermoplastic starch-waxy maize starch nanocrystals nanocomposites," *Biomacromolecules*, vol. 7, no. 2, pp. 531–539, 2006.

[39] N. Ljungberg, J.-Y. Cavaillé, and L. Heux, "Nanocomposites of isotactic polypropylene reinforced with rod-like cellulose whiskers," *Polymer*, vol. 47, no. 18, pp. 6285–6292, 2006.

[40] J. D. D. Melo, L. F. M. Carvalho, A. M. Medeiros, C. R. O. Souto, and C. A. Paskocimas, "A biodegradable composite material based on polyhydroxybutyrate (PHB) and carnauba fibers," *Composites Part B*, vol. 43, no. 7, pp. 2827–2835, 2012.

[41] C. McCann, "The measurement of the sizes of non-spherical particles by the hydrometer method," *Sedimentology*, vol. 13, pp. 307–309, 1969.

[42] C. N. Quiroz-Reyes, E. Ronquillo-De Jesús, N. E. Duran-Caballero, and M. Á. Aguilar-Méndez, "Development and characterization of gelatin nanoparticles loaded with a cocoa-derived polyphenolic extract," *Fruits*, vol. 69, no. 6, pp. 481–489, 2014.

[43] K. Zhao, Y. Deng, J. C. Chen, and G.-Q. Chen, "Polyhydroxyalkanoate (PHA) scaffolds with good mechanical properties and biocompatibility," *Biomaterials*, vol. 24, no. 6, pp. 1041–1045, 2003.